International Journal of Heat and Technology
Vol. 40, No. 2, April, 2022, pp. 592-598
Journal homepage: http://iieta.org/journals/ijht

Regional Construction and Differences of Thermal Environment in Vernacular Buildings

Juan Chen[1,2], Jianrong Yang[3*]

[1] Department of Art and Design, Anhui University of Arts, Hefei 230001, China
[2] Faculty of Decorative Arts, Silpakorn University, Bangkok 10200, Thailand
[3] College of Art and Design, Hunan First Normal University, Changsha 410205, China

Corresponding Author Email: yangjianrong@hnfnu.edu.cn

https://doi.org/10.18280/ijht.400228

Received: 15 December 2021
Accepted: 24 February 2022

Keywords:
vernacular buildings, regional construction of thermal environment, differences

ABSTRACT

Unlike the traditional extensive heating management, the on-demand precise time- and region-specific heating strategy can effectively reduce the heating energy consumption of vernacular buildings. The existing studies on the time- and region-specific heating strategy of vernacular buildings face several problems: the time and space are not clearly divided, the heating model cannot simultaneously satisfy the different heating demands of residents in different periods, and the proper time- and region-specific heating terminals are severely lacking. To solve these problems, this paper explores the regional construction and differences of thermal environment in vernacular buildings. Firstly, we classified the regional construction of thermal environment in vernacular buildings, analyzed the thermal process for the regional construction, and determined the implementation model for heating actual vernacular buildings. The layout of rooms inside a multi-space vernacular building determines the difference in heat gain and loss between the rooms to be heated, when the heating system operates naturally. With this in mind, we analyzed the regional thermal balance of thermal environment in vernacular buildings, linearly fitted the average indoor thermal sensation in each region of a vernacular building in day and night, and obtained the relevant experimental results. In addition, the regional indoor temperature changes were summarized at different glazing ratios and different roof heat transfer resistances. The results show the effectiveness of the regional construction strategy of thermal environment based on time and regional differences.

1. INTRODUCTION

All buildings in the vernacular environment can be called vernacular buildings, which manifest the local spirit and local culture in the passage of time [1-8]. Regionally speaking, vernacular buildings are the buildings related to the production and life in rural areas, which differ from urban buildings [9-13]. Thanks to economic development, the living conditions of rural residents have been significantly improved. But there are still many problems with vernacular buildings. For example, the building envelopes have a poor thermal performance; the thermal environment cannot be constructed easily in winter; the heating system is imperfect, difficult to upgrade/transform, and likely to seriously pollute indoor air [14-23]. Unlike the traditional extensive heating management, the on-demand precise time- and region-specific heating strategy can effectively reduce the heating energy consumption of vernacular buildings. Based on the law of indoor activity trajectories and the difference of heating between different periods in vernacular buildings, it is very meaningful to explore the on-demand precise time- and region-specific heating management.

The constant changes of environmental conditions add to the difficulty in analyzing the actual thermal state of buildings. Malinowski and Muzychak [22] proposed a methodological approach to overcome the difficulty, and mathematically modeled the thermal state of buildings. Based on a power circuit, the model depicts all components of heat loss and heat gain. Through thermal state analysis, their model can simultaneously obtain the energy index of the building, and capture an objective image of the thermal comfort of the room. Using Airpak, Yu et al. [23] simulated the thermal environment of the office with three air supply angles (0°, 45°, and 60°) of the cabinet air conditioner in summer. The simulated indoor airflow velocity distribution and temperature distribution were analyzed, revealing that the thermal comfort of the room is optimal, when the air is supplied at an upward angle of 45°. During the design phase, the simulated energy consumption is often taken as a metric of residential building performance. For free-running buildings, EC may not be an appropriate metric due to the absence of heating/cooling equipment. Zhou et al. [24] characterized the long-term indoor thermal environment with thermal discomfort rate (TDCR), and examined the impact of different evaluation indices on building performance. The results show that, when the envelope design is changed, energy consumption is strongly correlated with TDCR, but the two indices have different trends and sensitivities. Yang et al. [25] conducted a field study on the thermal comfort conditions of residential buildings in high-latitude sub-atmospheric pressure regions in China. The summer research covers 33 people in 25 residential units, and the winter research covers 43 people in 20 residential units. A subjective questionnaire survey was carried out on thermal sensation vote (TSV), followed by an objective field measurement. Thermal environmental problems are widespread among urban high-rise buildings.

Zhang et al. [26] analyzed this phenomenon in the light of the effects of different types of wall materials. Computational fluid dynamics (CFD) was adopted to simulate the thermal environment of a typical urban residential community, and the simulation data were carefully analyzed. Some useful results were drawn through the research: The direction of the building has a great impact on the air circulation, and the north-south is the best direction.

The existing studies on time- and region-specific heating strategy mainly tackle the heating technology, thermal demand, and heating terminal form. Most problems in thermal environment creation of vernacular buildings can already be solved. However, the following problems need to be solved urgently: the time and space are not clearly divided, the heating model cannot simultaneously satisfy the different heating demands of residents in different periods, and the proper time- and region-specific heating terminals are severely lacking. To solve these problems, this paper explores the regional construction and differences of thermal environment in vernacular buildings. The main contents are as follows: (1) Section 2 classifies the regional construction of thermal environment in vernacular buildings, analyzes the thermal process for the regional construction, and determines the implementation model for heating actual vernacular buildings. (2) The regional thermal balance of thermal environment in vernacular buildings was analyzed in the light of the following rule: The layout of rooms inside a multi-space vernacular building determines the difference in heat gain and loss between the rooms to be heated, when the heating system operates naturally. (3) We linearly fitted the average indoor thermal sensation in each region of a vernacular building in day and night, and obtained the relevant experimental results. (4) The regional indoor temperature changes were summarized at different glazing ratios and different roof heat transfer resistances. The results show the effectiveness of the regional construction strategy of thermal environment based on time and regional differences.

2. THERMAL PROCESS ANALYSIS

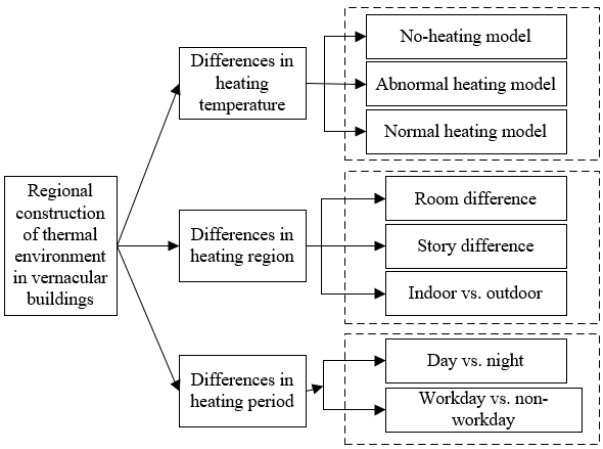

Figure 1. Classification of regional construction of thermal environment in vernacular buildings

The regional construction strategy of thermal environment in vernacular buildings can be divided according three criteria (see Figure 1): differences in heating period. differences in heating region, and differences in heating temperature. The differences in heating period include day vs. night, and workday vs. non-workday; the differences in heating region include room difference, story difference, and indoor vs. outdoor; the differences in heating temperature include no-heating model, abnormal heating mode, and normal heating model. To determine the implementation model for heating actual vernacular buildings, this study further explores the creation of different thermal environments.

Firstly, we analyzed the thermal process of regional construction of thermal environment in vernacular buildings. In a vernacular building, the thermodynamic system of each room can be regarded as the interior space enclosed by the inner surface of the envelope and the indoor air. Thus, the thermal environment of the room can be characterized by the thermal balance equation of the inner surface of the building envelope and the heat balance equation of the indoor air.

The time- and region- specific heating model divides the thermal process of the thermal environment construction for the rooms in a vernacular building into three stages: adjustment stage, intermittent stage, and preheating stage. Next, we would construct the thermal balance equation of each stage. In the vernacular building, thermal balance is achieved on the inner surface of the envelope structure of each room. That is, the sum of the following four heats equals zero: the radiation heat directly borne by the inner surface of each envelope structure, the mutual radiation heat between the inner surfaces, the conducted heat between the inner surfaces, and the convective heat of the indoor air.

Let $p_s(m)$ be the room temperature; $p_i(m)$, and $p_l(m)$ be the inner surface temperatures of the i-th and l-th envelopes, respectively; β^d_i be the convective heat transfer coefficient of the inner surface of the i-th envelope; D_y be the Stefan-Boltzmann constant; σ_{il} be the system blackness between the inner surfaces of the i-th and l-th envelopes (σ_{il} is approximately equal to the product between the surface blackness of the two surfaces: $\sigma_{il} \approx \sigma_i \sigma_l$); ψ_{il} is the radiation angle coefficient of inner surface of the i-th envelope to the inner surface of the l-th envelope; M_i be the total number of inner surfaces of different envelopes of the room; $w_i(m)$ be the temperature difference between the two sides; $w_i^s(m)$ be the sum of the convective heat gain, directly obtained solar radiation heat, and the radiation heat of various internal disturbances of the inner surface of the i-th envelope. Then, the thermal balance of the i-th surface per unit area at time m can be expressed as:

$$\begin{aligned} & w_i(m) + \beta_i^d \left[p_l(m) - p_i(m) \right] \\ & + \sum_{l=1}^{M_i} D_y \sigma_{il} \psi_{il} \left[\left(\frac{P_l(m)}{100} \right)^4 - \left(\frac{P_i(m)}{100} \right)^4 \right] \\ & + w_i^s(m) = 0 \end{aligned} \tag{1}$$

In vernacular buildings, the envelope structure usually has a certain heat storage capacity. The radiation heat borne by the structure is under time-varying disturbances. As a result, the thermal balance equation is a set of differential equation, which should be solved by transforming the coefficients of heat transfer and inner/external surface absorption, or using the reaction coefficient method. Let μ_i be the heat transfer coefficient of the inner surface of the thermally inert slab envelope; ξ be the a-coordinate value of the inner surface of this type of envelope; M_j be the total number of inner surfaces of thermally inert slab envelopes in the room. For a thermally

inert slab envelope, we have:

$$w_i(m) = \mu_i \frac{\partial p}{\partial a}|_{a=\xi} \tag{2}$$

Let L_i be the heat transfer coefficient of the i-th door/window; β_i be the total heat transfer coefficient of the inner surface of the i-th envelope. Without considering the heat storage of doors and windows, the following holds for the envelope:

$$w_i(m) = \frac{1}{\frac{1}{L_i} - \frac{1}{\beta_i}} \left[p_{\beta i}(m) - p_i(m) \right] \tag{3}$$

Let β^s_i be the radiation heat transfer coefficients between inner surfaces of envelopes i and l. The mutual radiation between inner surfaces of the vernacular building can be calculated by:

$$\begin{aligned} &\sum_{l=1}^{M_i} D_y \sigma_{il} \psi_{il} \left[\left(\frac{P_l(m)}{100} \right)^4 - \left(\frac{P_i(m)}{100} \right)^4 \right] \\ &= \sum_{l=1}^{M_i} \beta^s_{il} \left[p_l(m) - p_i(m) \right] \end{aligned} \tag{4}$$

β^s_i satisfies:

$$\begin{aligned} \beta^{'}_{il} &= D_y \sigma_{il} \psi_{il} \frac{\left(\frac{P_l(m)}{100} \right)^4 - \left(\frac{P_i(m)}{100} \right)^4}{p_l(m) - p_i(m)} \\ &\approx 4 \times 10^{-8} D_y \sigma_{il} \psi_{il} \left[P_n(m) \right]^3 \end{aligned} \tag{5}$$

Let $RFO^E_i(m)$ be the heat gain from the direct solar radiation projected onto the i-th inner surface at time m; $RFO_e(m)$ e the heat gain from the total solar radiation projected into the room at time m; $FO_k(m)$ be the heat gain from lighting at time m; $FO_{yr}(m)$ be the heat gain from the sensible heat of indoor residents at time m; $FO_{xr}(m)$ be the heat gain from the sensible heat of equipment at time m; D_k, D_y, and D_x be the percentage of the convective part in the heat gain from lighting, indoor residents, and equipment, respectively; G_l, and G_i be the inner surface areas of the l-th and i-th envelopes, respectively. At time m, the radiation heat gain w^s_i of the inner surface of an envelope can be calculated by:

$$\begin{aligned} w^s_i = &\frac{\begin{array}{l} RFO_e(m) + FO_k(m)(1 - D_k) \\ +FO_{yr}(m)(1 - D_y) + FO_{xr}(m)(1 - D_x) \end{array}}{\sum_{l=1}^{M_i} G_l} \\ &+ \frac{RFO^E_i}{G_i} \end{aligned} \tag{6}$$

In the vernacular building, the air must be circulatable in the rooms to be heated. Thus, the heat transfer process is dynamic. That is, the sum of convective heat transfer between indoor air and the inner surface of each envelope, the convective heat gain of indoor air, the infiltration heat gain of outdoor air, and the heat supply of the heating system equals the sensible heat reduction of the air in the room to be heated per unit time.

Suppose the convective heat loss w^d_1 from lighting, sensible heat of indoor resident, and sensible heat of equipment at time m satisfies $w^d_1 = FO_k D_k + FO_{yr} D_y + FO_{xr} D_x$. Let w^d_2 be the sensible heat of the room consumed by the heat absorption for water evaporation at time m; $K(m)$ be the air infiltration amount at time m; $(d\varphi)_x$, $(d\varphi)_s$ be the unit heat capacity of the air; x and s be the subscripts of outdoor and indoor environments, respectively; U be the volume of the room; $FZ(m)$ be the heat supply per unit time. Then, the dynamic thermal balance of indoor air in the room to be heated of a vernacular building at time m can be expressed as:

$$\begin{aligned} &\sum_{l=1}^{M_i} G_l \beta^d_i \left[p_l(m) - p_s(m) \right] \\ &+ \left[w^d_1(m) - w^d_2(m) \right] + Kx(m)(d\phi)_x \\ &\left[p_l(m) - p_s(m) \right] / 3.6 + FZ(m) \\ &= U(d\phi)_s \frac{p_s(m-1) - p_s(m)}{3.6 \times \Delta\upsilon} \end{aligned} \tag{7}$$

Formulas (1) and (7) can be combined into the set of thermal balance equations for the room to be heated. During the preheating stage and adjustment stage, the heat supply of the heating system, and the inner surface temperature variation of each indoor envelope at any time can be derived from the indoor temperature at that time. During the intermittent stage, the heating system comes to a standstill. Then, the indoor temperature variation of the vernacular building, as well as the initial temperature of the preheating stage, can be solved by the proposed set of indoor thermal balance equations. Based on the preset indoor temperature for each time, it is possible to compute the indoor preheating load of the vernacular building at any time.

For the vernacular building envelopes, the indoor temperature in the heat transfer governing equation changes continuously, while the solutions of the proposed equation set are discrete. Therefore, the boundary conditions of the indoor and outdoor air temperatures in vernacular buildings should undergo discrete fitting.

It is assumed that $p_s = g(\upsilon)$. Then, the period of $0 \sim \upsilon$ was split into n segments with an interval of $\Delta\upsilon$. The moment of step change was denoted as time m, which satisfies $\upsilon_m = m\Delta\upsilon$. Then, $p_s = g(\upsilon)$ was divided into n step reactions. Let $v(\upsilon)$ be a unit step function. Then, we have:

$$\begin{aligned} g(\upsilon) &= g(0)\omega(0) \\ &+ \sum_{m=1}^{n} \left[g(\upsilon_m) - g(\upsilon_{m-1}) \right] v(\upsilon - \upsilon_m) \end{aligned} \tag{8}$$

$v(\upsilon)$ can be defined as:

$$v(\upsilon) = \begin{cases} 1, \upsilon \geq 0 \\ 0, \upsilon < 0 \end{cases} \tag{9}$$

If $n \to \infty$, we have:

$$g(\upsilon_m) - g(\upsilon_{m-1}) = \frac{dg(\upsilon)}{d\upsilon} \Delta\upsilon \big|_{\upsilon=\upsilon_m} \tag{10}$$

When υ_s changes continuously, the internal temperature distribution of the one-dimensional (1D) envelope in the vernacular building can be expressed as:

$$\begin{aligned} & p(a,\upsilon) = g(a,0)\omega(a,0) \\ & + \sum_{m=1}^{n} \left[g(a,\upsilon_m) - g(a,\upsilon_{m-1}) \right] \omega(a,\upsilon-\upsilon_m) \\ & = g(a,0)\omega(a,0) + \int_0^{\upsilon} \frac{dg(\upsilon)}{d\upsilon} \omega(a,\upsilon-\upsilon_m) d\upsilon \end{aligned} \tag{11}$$

If the boundary conditions of the indoor and outdoor air temperatures in the rooms to be heated in the vernacular building are continuous, then Duhamel's principle was adopted to solve these conditions.

To characterize the feature factors of heat load in vernacular buildings, the thermal balance equations of the rooms to be heated can be combined to obtain:

$$FZ(m) = g\begin{bmatrix} w_i, w_i^s, w_1^d, w_2^d, x_i^d, p_i(m), \\ p_s(m), p_s(m-1), p_c, K_x, U, \upsilon \end{bmatrix} \tag{12}$$

Formula (12) shows that the indoor heat load of vernacular buildings is affected by the following factors: the size and thermal performance of the envelope, outdoor air temperature, directly received solar radiation intensity, preset target indoor temperature, heating model, heat transfer between adjacent rooms, and preheating duration.

3. THERMAL BALANCE ANALYSIS

The layout of rooms inside a multi-space vernacular building determines the difference in heat gain and loss between the rooms to be heated, when the heating system operates naturally. As a result, the air temperature varies with rooms. If there is a temperature difference between adjacent rooms in the vernacular building, these room will transfer heat via the common wall. For a multi-space vernacular building, the heat transfer between adjacent rooms is nonnegligible.

Let w_{dd} be the passive heat collection per unit floor area; $w_{U\cdot F}$ be the internal heat gain per unit floor area; $w_{F\cdot P}$ be the heat transfer per unit floor area via the envelope structure; w_{AMG} be the heat loss of air infiltration per unit floor area. During the heating season, the steady-state thermal balance of the vernacular building can be expressed as:

$$w_{dd} + w_{A\cdot F} - w_{F\cdot P} - w_{AMG} = 0 \tag{13}$$

Let $X_{0\cdot j}$ be the indoor area of the j-th room of the vernacular building; $S_{1\cdot M\cdot b\cdot j}$ be the heat transfer resistance of the partition wall between the j-th room and the adjacent room b; $S_{0\cdot Q\cdot a\cdot j}$, $S_{2\cdot S\cdot a\cdot j}$, $S_{0\cdot O\cdot j}$, and $S_{0\cdot eQ\cdot c\cdot j}$ be the heat transfer resistances of the outer wall, roof, floor, and doors/windows of room a, respectively; $G_{Q\cdot a\cdot j}$ be the area of the partition wall between the j-th room and the adjacent room b; $G_{Q\cdot a\cdot j}$, $G_{eQ\cdot cj}$, $G_{S\cdot j}$, and $G_{O\cdot j}$ be the areas of the outer wall, roof, floor, and doors/windows of room a, respectively; Δp_{bj}^* be the temperature difference between the j-th room and the adjacent room b; $p_{rx\cdot a\cdot j}^*$ be the mean composite outdoor temperature of the heating season corresponding to the outer wall; $p_{rx\cdot S\cdot j}^*$ be the mean composite outdoor temperature of the heating season corresponding to the horizontal plane; SH_T^* be the mass specific heat capacity of dry air at constant pressure; σ be the density of outdoor air; M be the number of ventilations; U be the ventilation volume; n, m, and k be the number of the partition walls between the j-th room and the adjacent room b, the number of outer walls of room a, and the number of doors and windows, respectively. Then, the steady-state thermal balance of the j-th room in the vernacular building can be expressed as:

$$\begin{aligned} & w_{dd\cdot j} \cdot X_{0\cdot j} + 3.8 X_{0\cdot j} \\ & + \sum_{b=1}^{n} \frac{1}{S_{1\cdot M\cdot b\cdot j}} G_{Q\cdot b\cdot j} \Delta p_{bj}^* \\ & - \sum_{a=1}^{m} \frac{1}{S_{0\cdot Q\cdot a\cdot j}} G_{Q\cdot a\cdot j} \left(p_{i\cdot j}^* - p_{rx\cdot a\cdot j}^* \right) \\ & - \sum_{c=1}^{k} \frac{1}{S_{0\cdot eq\cdot c\cdot j}} G_{eq\cdot c\cdot j} \left(p_{i\cdot j}^* - p_z^* \right) \\ & - \frac{1}{S_{2\cdot S\cdot j}} G_{S\cdot j} \left(p_{i\cdot j}^* - p_{rx\cdot S\cdot j}^* \right) \\ & - \frac{1}{S_{0\cdot O\cdot j}} G_{O\cdot j} \left(p_{i\cdot j}^* - p_z^* \right) \\ & - \left(d_t \phi M U_j \right) \left(p_{i\cdot j}^* - p_d^* \right) = 0 \end{aligned} \tag{14}$$

Let GR_N be the daily average total radiation on the south façade of the vernacular building; C_N be the ratio of the daily average total radiation on the south façade through the glass to the daily average total radiation on the south façade; β_x be the ratio of the daily average total radiation absorbed by the vernacular building through the glass to the daily average total radiation through the glass; X_h be the area of glass windows; A_n be the effective light transmission area coefficient of the glass windows. Then, the passive heat collection per unit floor area $w_{dd,\,j}$ of the j-th room in the vernacular building can be calculated by:

$$w_{dd,j} = GR_N \cdot \upsilon_N \cdot \beta_x \cdot X_h \cdot A_n \tag{15}$$

4. EXPERIMENTS AND RESULTS ANALYSIS

The heating system combines heatable brick bed with underfloor heating. Our experiments target a vernacular building in Maojia Village, Siqian Township, Guangze County, Nanping City, southeastern China's Fujian Province. The building contains five rooms: bedroom 1 (Region A), bedroom 2 (Region B), restroom (Region C), living room (Region D), and kitchen (Region D). All rooms have the same interior height, envelope size, and envelope structure. Figure 2

shows the plan of the vernacular building. The specific structure and size of the envelope can be inferred from the plan.

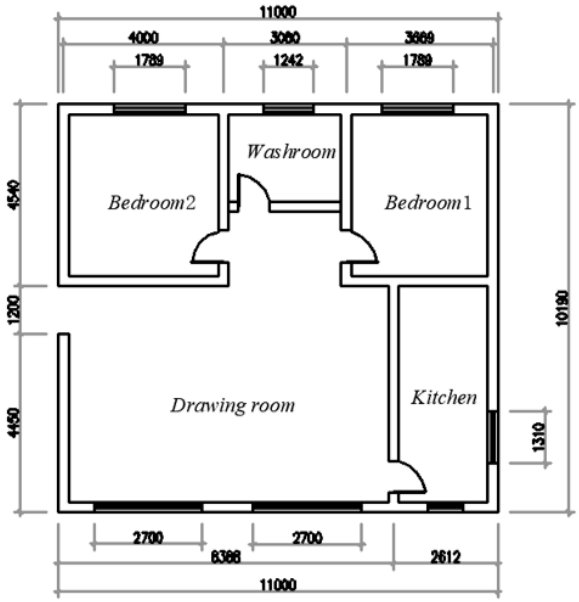

Figure 2. Plan of the test building

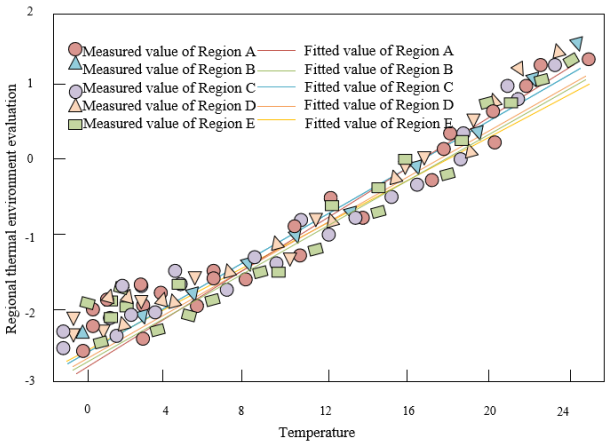

Figure 3. Indoor thermal environment evaluation of each region in day

Table 1. Linearly fitted average indoor thermal sensation in each region in day

Region number	A	B	C	D	E
R^2	0.947	0.925	0.931	0.948	0.847
Neutral temperature	17.3	16.8	17.2	17.4	16.5
Range of comfortable temperature	13.8-21.4	13.6-21.7	13.5-21.1	13.6-20.4	13.5-21.7

Based on Bin's method, this study linearly fits the average indoor thermal sensation in each region of the vernacular building in day. The results are displayed in Figure 3 and Table 1. It can be inferred that, during the day, the average indoor thermal sensation in each region of the building fluctuated by a similar magnitude as indoor temperature. The regression coefficient was about 0.13. The different regions had similar average indoor thermal sensations in day, i.e., the residents in the area of the building are not sensitive to the changes of room temperature. Based on the fitting results of Figure 3, we further derived the regression equation for the average indoor thermal sensation in each region in day. According to the neutral temperature and range of comfortable temperature in Table 1, the different regions differed slightly in neutral temperature in day. The lowest neutral temperature appeared in the living room (Region D), due to the large area of that region. During the day, when the average indoor thermal sensation belonged to [-0.5, +0.5], the corresponding range of comfortable temperature should be 13.5~21.0°C.

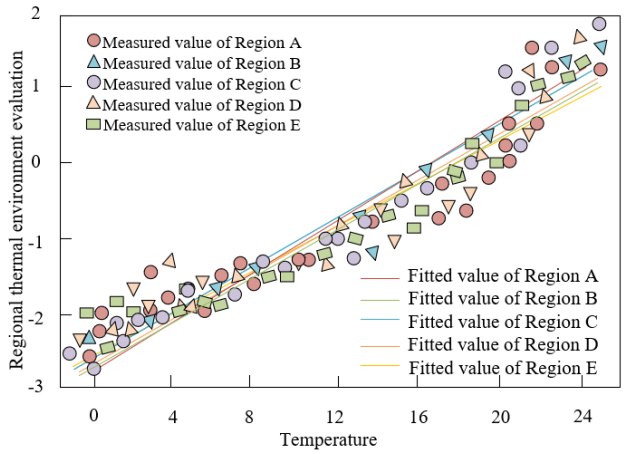

Figure 4. Indoor thermal environment evaluation of each region at night

Table 2. Linearly fitted average indoor thermal sensation in each region at night

Region number	A	B	C	D	E
R^2	0.942	0.968	0.905	0.972	0.948
Neutral temperature	11.3	12.7	12.3	12.2	11.9
Range of comfortable temperature	9.2-15.7	8.5-15.2	8.2-14.9	8.5-14.9	8.2-15.4

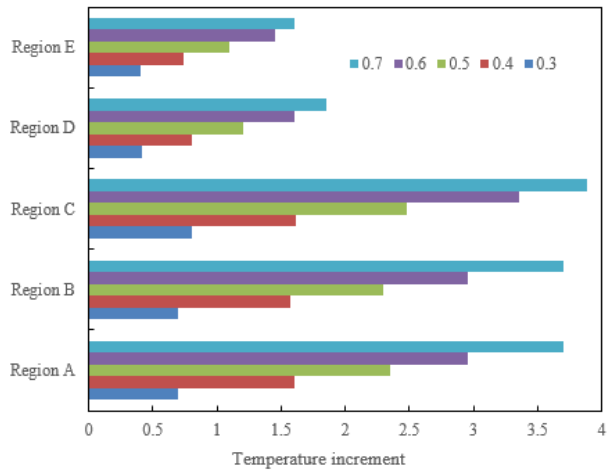

Figure 5. Indoor temperature variation in each region at different glazing ratios

Figure 4 and Table 2 present the linearly fitted average indoor thermal sensation in each region of the vernacular building at night. The results show that, with the changes of room temperature, the average indoor thermal sensation in each region fluctuated slightly at night. The neutral temperature was 0.5~0.6°C lower than that in day. The

regression coefficient at night was smaller than that in day. The residents are less sensitive to room temperature variation, probably due to the adoption of insulation measures (e.g., covered with a quilt) at night. Hence, the vernacular building had a larger range of comfortable indoor temperature at night, which is [8.2,15.7], than in day.

Figure 5 shows the indoor temperature variation in each region at different glazing ratios. As the glazing ratio increased from 0.3 to 0.7, the average indoor temperatures in all regions of the vernacular building were on the rise, but the temperature increment varied significantly between regions. With the growing glazing ratio, the three regions in the north, namely, bedroom 1 (Region A), bedroom 2 (Region B), and restroom (Region C), saw greater increment of average indoor temperature than the two regions in the south, namely, living room (Region D) and kitchen (Region E). Although the vernacular building has a stable overall heat gain and loss, the proposed construction strategy for thermal environment distribution fully considers the time and regional differences, and realizes nonhomogeneous distribution of heat between the rooms. The supplied heat is concentrated in the 3 rooms in the north as much as possible, which effectively improves the temperature inside the two bedrooms.

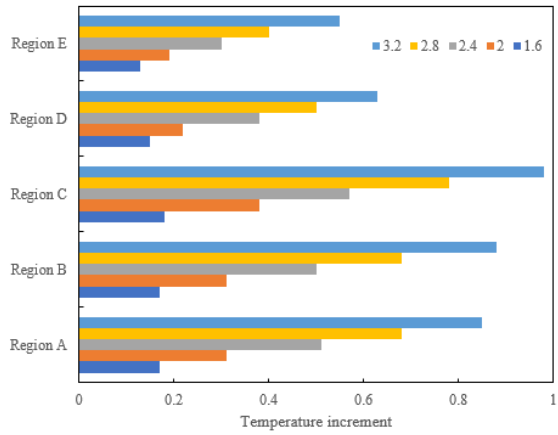

Figure 6. Indoor temperature variation in each region at different roof heat transfer resistances

Figure 6 shows the indoor temperature variation in each region at different roof heat transfer resistances. As the roof heat transfer resistance gradually rose from 1.6 to 3.2, the average indoor temperatures in all regions of the vernacular building were on the rise, but the temperature increment varied significantly between regions. With the growing roof heat transfer resistance, the three regions in the north, namely, bedroom 1 (Region A), bedroom 2 (Region B), and restroom (Region C), saw greater increment of average indoor temperature than the two regions in the south, namely, living room (Region D) and kitchen (Region E). The results further demonstrate the effectiveness of our time- and region-specific regional construction strategy for thermal environment.

5. CONCLUSIONS

This study mainly investigates the regional construction and differences of thermal environment in vernacular buildings. After classifying he regional construction of thermal environment in vernacular buildings, we analyzed the thermal process for the regional construction, and determined the implementation model for heating actual vernacular buildings. Then, the regional thermal balance of thermal environment in vernacular buildings was discussed, in the light of the following rule: the layout of rooms inside a multi-space vernacular building determines the difference in heat gain and loss between the rooms to be heated, when the heating system operates naturally. Through experiments, we linearly fitted the average indoor thermal sensation in each region of the vernacular building in day and at night, and obtained the corresponding ranges of comfortable temperature. In addition, the indoor temperature variation in each region was simulated at different glazing ratios and roof heat transfer resistances. The results show that, with the growth of glazing ratio and roof heat transfer resistance, the northern regions saw greater increment of average indoor temperature than the southern regions. The results demonstrate the effectiveness of our time- and region-specific regional construction strategy for thermal environment.

ACKNOWLEDGEMENT

Supported by the key project of Provincial Natural Science Foundation of Anhui Universities "Research on green construction strategy of Huizhou traditional human settlements from the perspective of Rural Revitalization" (Grant No.: KJ2021A1153).

REFERENCES

[1] Zaryoun, M., Hosseini, M., Soleymani, K. (2021). Sustainable architecture and earthquake resilience of vernacular Zegalli houses in northern Iran. Engineering, Construction and Architectural Management, 29(2): 1061-1085. https://doi.org/10.1108/ECAM-05-2020-0362

[2] Philokyprou, M., Michael, A. (2021). Environmental Sustainability in the Conservation of Vernacular Architecture. The Case of Rural and Urban Traditional Settlements in Cyprus. International Journal of Architectural Heritage, 15(11): 1741-1763. https://doi.org/10.1080/15583058.2020.1719235

[3] Amraoui, K., Sriti, L., Di Turi, S., Ruggiero, F., Kaihoul, A. (2021). Exploring building's envelope thermal behavior of the neo-vernacular residential architecture in a hot and dry climate region of Algeria. In Building Simulation, 14(5): 1567-1584. https://doi.org/10.1007/s12273-021-0764-0

[4] Li, Y., Zhu, Y., Yu, L., Bi, Z., Huang, G. (2021). Typology in vernacular architecture—Qianmo Tower Post Station in Mingyue village. In E3S Web of Conferences (Vol. 237). EDP Sciences. https://doi.org/10.1051/e3sconf/202123703019

[5] Elert, K., Baños, E.G., Velasco, A.I., Bel-Anzué, P. (2021). Traditional roofing with sandstone slabs: Implications for the safeguarding of vernacular architecture. Journal of Building Engineering, 33: 101857. https://doi.org/10.1016/j.jobe.2020.101857

[6] Caruso, M., García-Soriano, L. (2020). Old Rauma (Finland): Living and researching vernacular architecture. International Archives of the Photogrammetry, Remote Sensing and Spatial Information Sciences (Online), 44: 11-18. https://doi.org/10.5194/isprs-archives-XLIV-M-

1-2020-11-2020
[7] Korachy, M. (2020). Is the loss of vernacular architecture reversible? The case of Lahun Village in Egypt. The International Archives of Photogrammetry, Remote Sensing and Spatial Information Sciences, 44: 977-984. https://doi.org/10.5194/isprs-archives-XLIV-M-1-2020-977-2020
[8] Pennacchio, R., De Filippi, F., Bosetti, M., Aoki, T., Wangmo, P. (2022). Influence of traditional building practices in seismic vulnerability of Bhutanese vernacular rammed earth architecture. International Journal of Architectural Heritage, 16(3): 374-393. https://doi.org/10.1080/15583058.2020.1785044
[9] Eybye, B.T. (2020). Danish vernacular architecture: Sustainability as a preservation value. The International Archives of Photogrammetry, Remote Sensing and Spatial Information Sciences, 44: 211-218. https://doi.org/10.5194/isprs-archives-XLIV-M-1-2020-211-2020
[10] Widera, B. (2021). Comparative analysis of user comfort and thermal performance of six types of vernacular dwellings as the first step towards climate resilient, sustainable and bioclimatic architecture in western sub-Saharan Africa. Renewable and Sustainable Energy Reviews, 140: 110736. https://doi.org/10.1016/j.rser.2021.110736
[11] Zouaoui, M.A., Djebri, B., Capsoni, A. (2020). From point cloud to HBIM to FEA, the case of a vernacular architecture: Aggregate of the Kasbah of Algiers. Journal on Computing and Cultural Heritage (JOCCH), 14(1): 1-21. https://doi.org/10.1145/3418039
[12] Alkubaisi, S. (2021). Regenerative design method and its relation with vernacular architecture: Kurdish vernacular Architecture as a case study. In 2021 International Conference on Advance of Sustainable Engineering and its Application (ICASEA), pp. 206-212. https://doi.org/10.1109/ICASEA53739.2021.9733063
[13] Xi, P., Xiao, X., Jingxuan, S. (2021). A study on design strategies of vernacular architecture based on data analysis of community's architectural preference. In E3S Web of Conferences, 236: 05067. https://doi.org/10.1051/e3sconf/202123605067
[14] Zheng, G., Bu, W. (2018). Review of heating methods for rural houses in China. Energies, 11(12): 3402. https://doi.org/10.3390/en11123402
[15] Gao, X.L., Xia, R.J., Zhang, X.D., Shang, L.B., Xiangli, M.Q. (2021). A steady-state modeling method for direct expansion air conditioning systems. International Journal of Heat and Technology, 39(6): 1945-1950. https://doi.org/10.18280/ijht.390632
[16] Deng, M., Nie, Y., Lu, F., Ma, R., Yuan, Y., Shan, M., Yang, X. (2022). Pollutant emission performances of improved solid fuel heating stoves and future implications in rural China. Energy and Buildings, 257: 111810. https://doi.org/10.1016/j.enbuild.2021.111810
[17] Pawar, H., Sinha, B. (2022). Residential heating emissions (can) exceed paddy-residue burning emissions in rural northwest India. Atmospheric Environment, 269: 118846. https://doi.org/10.1016/j.atmosenv.2021.118846
[18] Xie, L., Hu, X., Zhang, X., Zhang, X. B. (2022). Who suffers from energy poverty in household energy transition? Evidence from clean heating program in rural China. Energy Economics, 106: 105795. https://doi.org/10.1016/j.eneco.2021.105795
[19] Soltero, V.M., Chacartegui, R., Ortiz, C., Velázquez, R. (2018). Potential of biomass district heating systems in rural areas. Energy, 156: 132-143. https://doi.org/10.1016/j.energy.2018.05.051
[20] Brocklebank, I., Beck, S., Styring, P. (2018). A simple approach to modeling rural and urban district heating. Frontiers in Energy Research, 103. https://doi.org/10.3389/fenrg.2018.00103
[21] Bücker, D., Jell, P., Botsch, R. (2018). Performance monitoring of rural district heating systems. Energy Procedia, 149: 5-14. https://doi.org/10.1016/j.egypro.2018.08.164
[22] Malinowski, A., Muzychak, A. (2018). Mathematical modeling of the building thermal state taking into account the heat and energy impact of the environment. In IOP Conference Series: Materials Science and Engineering, 415(1): 012047. https://doi.org/10.1088/1757-899X/415/1/012047
[23] Yu, W., Zhang, J., Li, H. (2018). Numerical Simulation and Analysis of Thermal Environment in Air-Conditioning Office Building. In IOP Conference Series: Earth and Environmental Science, 199(3): 032068. https://doi.org/10.1088/1755-1315/199/3/032068
[24] Zhou, J., Song, Y., Zhang, G. (2017). Correlation analysis of energy consumption and indoor long-term thermal environment of a residential building. Energy Procedia, 121: 182-189. https://doi.org/10.1016/j.egypro.2017.08.016
[25] Yang, L., Yan, H., Xu, Y., Lam, J.C. (2013). Residential thermal environment in cold climates at high altitudes and building energy use implications. Energy and Buildings, 62: 139-145. https://doi.org/10.1016/j.enbuild.2013.02.058
[26] Zhang, L., Huang, Y.H., Yang, L. (2013). Study on building engineering with simulation and analysis of outdoor thermal environment for a residential subdistrict in hot summer/cold winter region. In Advanced Materials Research, 700: 235-238. https://doi.org/10.4028/www.scientific.net/AMR.700.235